



ELSEVIER

Available online at www.sciencedirect.com

SCIENCE @ DIRECT®

Physica A 327 (2003) 378–398

PHYSICA A

www.elsevier.com/locate/physa

Quenched disorder and long-tail distributions

A. Kleczkowski^a, P.F. Góra^{b,*}

^a*Department of Plant Sciences, University of Cambridge, Cambridge CB2 3EA, UK*

^b*M. Smoluchowski Institute of Physics, Jagellonian University, Reymonta 4, 30-059 Kraków, Poland*

Received 28 October 2002

Abstract

A model of overdamped and externally stimulated oscillators is discussed. It is shown analytically that in the uncoupled case a wide class of random distributions of parameters of individual oscillators leads to a long-tail distribution of resting points. Interactions between the individual oscillators destroy these long tails partially (nearest-neighbours interaction) or completely (mean field interactions). As the levels of a local coupling increase, domains of similarly acting oscillators are formed. The collective behaviour becomes important for large local coupling at which the long tails are destroyed. In this case, the observed pattern of resting states is a reflection of both the quenched disorder and interactions between the oscillators.

© 2003 Elsevier B.V. All rights reserved.

PACS: 05.45.Ra; 87.23.Cc

Keywords: Long-tail distributions; Quenched disorder; Domains formation

1. Introduction

Power-law, or long-tail, distributions of various quantities have been observed in many systems, ranging from earthquakes [1], through evolving networks [2], coupled map lattices [3], percolation [4], avalanches [5] to distributions of company income and sizes [6], to quote just a couple of most recent results. A characteristic feature of such systems is an occurrence of large fluctuations with individual subsystems (or replicates) markedly differing from the rest. Although systems that exhibit power-law distributions are frequently observed, there is still no universally accepted framework which can explain the origin of the abundance and diversity of such distributions.

* Corresponding author.

E-mail addresses: adamk@mathbio.com (A. Kleczkowski), gora@if.uj.edu.pl (P.F. Góra).

It has been shown [7] that in some cases interactions among individual agents facilitate the emergence of the long tails. In other situations, a quenched disorder of initial parameters of the respective models plays a crucial role in a future evolution of the system. Variability in the transient behaviour, resulting from small differences in initial conditions or values of critical parameters, is then reflected in the final state [8]. We show that quenched parametric disorder can also be responsible for long-tail distributions.

In the present paper we discuss a system of overdamped and periodically stimulated particles (oscillators) whose behaviour is governed by two competing processes: The internal dynamics drives them to their natural resting points, while the external stimulation tries to destabilize these resting points. Such behaviour is quite common in practice and may lead to very interesting phenomena. In our case, individual oscillators differ from each other and their parameters are randomly drawn from a distribution. The oscillators may be independent (uncoupled) or may interact with each other; the former case corresponds to a statistical ensemble of non-identical individuals who obey identical dynamical laws.

The most interesting aspect of such a system is whether the oscillators go to non-trivial resting points, and if so, what is the final distribution of these resting points. We show analytically that in the uncoupled case a broad class of the parameter distributions leads to a long-tail distribution of resting points: A disorder in the parameters described by distributions frequently encountered in natural systems induces a distribution of resting points that is characterised by diverging moments. Typically, the distribution can be normalized, but even the mean is not properly defined. Moreover, we show that it is the oscillators for which the decay following the external stimulus is slowest that are responsible for the presence of the long tails.

If individual oscillators are coupled, collective effects may show up. We consider here two types of coupling: nearest neighbours and mean field type. With nearest neighbours coupling switched on, the distribution of resting points gets narrower, but still many oscillators tend to go to very large values, and the mechanism responsible for this is essentially the same as in the uncoupled case. When the coupling is of the mean field type, resting points of all oscillators lie in a narrow interval around the mean.

This paper is organized as follows: In Section 2 we introduce and motivate our model. In Section 3 we present analytical results for the uncoupled case and examples of typical resting points distributions. Numerical results for the coupled case are presented in Section 4. Possible applications of the formalism are briefly discussed in Section 5, and concluding remarks are given in Section 6.

2. The model

Let us assume that a single oscillator is described by a variable $y(t)$. The dynamics of $y(t)$ is split into two competing parts with very different time scales. A slow process is generated by an overdamped motion in a simple harmonic potential with a stable

fixed point at $y = 0$ so that

$$\frac{dy}{dt} = -\lambda y. \quad (1)$$

We assume that at times $t = t_n$, $n = 1, 2, \dots$ the motion is interrupted by a fast process. The perturbation is strictly limited in time, and the amplitude of the modification is scaled appropriately so that the effect of it is finite. The sequence $\{t_n\}_{n=1}^{\infty}$ can be either periodic, $t_n = n\tau$, or random. In this paper we consider the first case only. Thus, we assume that the dynamics of $y(t)$ is governed by the equation

$$\frac{dy}{dt} = -\lambda y + \varepsilon \sum_n \delta(t - n\tau)g(y). \quad (2)$$

$\varepsilon > 0$ is introduced to simplify the manipulation of the (integrated) strength of a pulse. Between the pulses $y(t)$ simply decays so that

$$y(n\tau^-) = e^{-\lambda\tau}y((n-1)\tau^+). \quad (3)$$

Because $y(t)$ undergoes a discontinuous jump at the pulse, Eq. (2) must be solved with an utmost care [9,10]. We have shown in Ref. [9] that the value after the n th pulse $y(n\tau^+)$ is related to the value just before this pulse $y(n\tau^-)$ by an implicit relationship

$$\int_{y(n\tau^-)}^{y(n\tau^+)} \frac{dy}{g(y)} = \varepsilon. \quad (4)$$

Assuming that (4) can be solved, we can formally write the solution as

$$y(n\tau^+) = y(n\tau^-) + \varepsilon\Phi(y(n\tau^-)). \quad (5)$$

In general $\Phi(y) \neq g(y)$. (3) and (5) together yield a stroboscopic formulation of the problem (2) ($y_n \equiv y(n\tau^+)$):

$$y_n = e^{-\lambda\tau}y_{n-1} + \varepsilon\Phi(e^{-\lambda\tau}y_{n-1}). \quad (6)$$

The first term on the right-hand side of Eqs. (2) and (6) describes the decay between pulses. Second term describes the influence of an external stimulation.

As the primary purpose of the in-pulse modification is to destabilize the stationary point $y = 0$, we assume that $\partial g(y)/\partial y > 0$ for $y \rightarrow 0$. In addition, in this paper we assume that asymptotically the force acting on the particle during the pulse does not depend on the position of the particle so that $g(y) \rightarrow \text{const}$ for $y \rightarrow \infty$, and the function $g(y)$ is a monotonic function of y . Sometimes it is more natural to define the effect of the pulse on the level of the stroboscopic map by specifying $\Phi(y)$ in (5). The latter case may occur when the impulse summarizes in an “artificial” time of finite steps a process that can take a considerable “real” time. The dynamics during the pulse differs considerably from the free evolution (1) although the pulse does not need to be short. Then, the starting point of the analysis is the stroboscopic map (6) itself rather than an equation of motion (2). In the following we will consider fairly general forms

of Φ , but specific results will be given for two cases: a state-independent pulse

$$y_n = zy_{n-1} + \varepsilon \tag{7}$$

(here and in the following $z \equiv e^{-\lambda\tau}$), which we call model A, and an asymptotically state-independent pulse

$$y_n = zy_{n-1} + \varepsilon \frac{zy_{n-1}}{1 + \alpha zy_{n-1}}, \tag{8}$$

which we call model B. $\Phi(y) = y/(1 + \alpha y)$ is well known in enzyme kinetics as a Michaelis–Menton relationship; α is a parameter determining the transition between a low- y and high- y behaviour of the map.

In the above, we considered a deterministic behaviour of a single particle. When an ensemble of such particles is introduced, the properties of the replicates may vary: The properties of the harmonic potential, λ , the strength of the perturbing field, ε , the frequency of the pulses, τ , and the additional parameters like α may be different in different oscillators. Instead of using constant (deterministic) values of the parameters, we will use random numbers drawn from certain probability distributions. Thus, we will consider a set of stroboscopic maps for variables $y_n(i)$ labelled by an index i ,

$$y_n(i) = z(i)y_{n-1}(i) + \varepsilon\Phi_i(z(i)y_{n-1}(i)), \tag{9}$$

where $z(i) = \exp(-\lambda(i)\tau(i))$ and the function Φ_i has the same form for all i . We allow $\lambda(i)$ and $\tau(i)$ to vary within a population, keeping all other parameters at fixed (deterministic) values. Note that τ is the interval between external stimuli, and $y_n(i)$ is the value of the i th oscillator just after the n th stimulus. In the uncoupled case it is possible that different oscillators are stimulated with different periods; this is equivalent to considering an ensemble of single oscillators differing, among others, in their stimulation periods. However, when the coupling is switched on (see below), stimulation periods of all oscillators must be equal for the sake of a model consistency. Therefore, considering τ to be a stochastic variable is meaningful only in the uncoupled case.

An obvious extension of the model is to consider coupling between individual particles. In this paper we assume that the coupling occurs during the pulse and is through a harmonic potential connecting two individual particles. We assume that the minimum of this potential corresponds to the resting case of the system without the pulsed perturbation (commensurate phase). Thus the map (9) becomes

$$x_n(i) \equiv z(i)y_{n-1}(i), \tag{10a}$$

$$y_n(i) = x_n(i) + \varepsilon(i)\Phi_i(x_n(i)) - \sum_j \frac{k_{ij}}{N_i}(x_n(i) - x_n(j)), \tag{10b}$$

where N_i is the number of oscillators for which $k_{ij} \neq 0$. We consider two cases of coupling: The local coupling corresponds to the nearest neighbours interaction $k_{ij} \sim \delta_{i,i-1} + \delta_{i,i+1}$, and the global coupling in which every particle is connected to every other particle with $k_{ij} = k = \text{const}$.

3. The uncoupled case

If there is no coupling, our model reduces to a collection of maps

$$y_{n+1} = e^{-\lambda\tau} y_n + \varepsilon\Phi(e^{-\lambda\tau} y_n), \tag{11}$$

where we have dropped the indices (*i*) for brevity. Parameters $\lambda > 0$ and $\tau > 0$ may differ among the oscillators, but formal expressions for the evolution of each oscillator are the same. To model the differences between individual oscillators, we assume that λ is a random number drawn from a certain distribution $P_\lambda(\lambda)$. We first need to find a distribution of the random variable

$$z = e^{-\lambda\tau}. \tag{12}$$

For the distribution of z we obtain

$$\begin{aligned} P_z(z) &= \int_0^\infty \delta(e^{-\lambda\tau} - z) P_\lambda(\lambda) d\lambda = \int_0^1 \delta(u - z) P_\lambda\left(-\frac{\ln u}{\tau}\right) \frac{du}{\tau u} \\ &= \frac{1}{z\tau} P_\lambda\left(-\frac{\ln z}{\tau}\right). \end{aligned} \tag{13}$$

It is easy to verify that $0 < z < 1$ is a necessary condition for $P_z(z)$ not to vanish identically.

The most interesting feature of (11) is that it can have a fixed point, satisfying

$$y^* = zy^* + \varepsilon\Phi(zy^*). \tag{14}$$

This equation can be formally solved, $y^* = F(z)$. Since z is a random variable, so is y^* . Assuming that F can be inverted, at least locally, for a distribution of the fixed points we obtain

$$P(y^*) = \int_0^1 \delta(y^* - F(z)) P_z(z) dz = \frac{1}{\tau z^*} \left(\frac{dF}{dz} \Big|_{z=z^*} \right)^{-1} P_\lambda\left(-\frac{\ln z^*}{\tau}\right), \tag{15}$$

where (13) has been used and $z^* = F^{-1}(y^*)$.

The fixed point y^* can assume a large value only if there is little decay between the pulses: y^* can be large only if z is slightly below unity. Thus $\zeta = 1 - z$ must be small and positive for $y^* \rightarrow \infty$. In this limit, (14) is equivalent to

$$\zeta y^* = \varepsilon\Phi(y^* - \zeta y^*). \tag{16}$$

We expand the right-hand side of (16) to the first order in ζ and obtain

$$\zeta \simeq \frac{\varepsilon\Phi(y^*)}{y^*(1 + \varepsilon \frac{d\Phi}{dy} |_{y=y^*})}. \tag{17}$$

Now assume that z approaches unity as

$$1 - z = \zeta \simeq \frac{\beta}{(y^*)^s} \tag{18}$$

with $s \geq 1$. In order for Eq. (17) to be consistent with (18) we need to have

$$\frac{\varepsilon\Phi(y^*)}{1 + \varepsilon \frac{d\Phi}{dy}|_{y=y^*}} \simeq \frac{\beta}{(y^*)^{s-1}} \tag{19}$$

for $y^* \rightarrow \infty$. If $\Phi(y)$ has, at least asymptotically for $y \rightarrow \infty$, a form

$$\Phi(y) = \frac{S(y)}{y^\eta Q(y) + R(y)}, \tag{20}$$

where $S(y)$, $Q(y)$, $R(y)$ are polynomials of arbitrary degrees n , m , and l , respectively, with $n \leq l \leq m$, and $0 \leq \eta < 1$, (19) is satisfied, provided that $s = m - n + \eta + 1$. In this case $\Phi \sim y^{-s+1}$ and $1 + \varepsilon d\Phi/dy$ behaves like $O(1)$.

In the $y^* \rightarrow \infty$ regime we can replace the right-hand side of (14) by its asymptotic form

$$(1 - z)y^* = \frac{\beta}{(zy^*)^{s-1}}. \tag{21}$$

We differentiate with respect to z and obtain

$$s(y^*)^{s-1} \frac{dy^*}{dz} = \beta \frac{sz - (s - 1)}{z^s(1 - z)^2}. \tag{22}$$

Now we use (18) and arrive at

$$\frac{dy^*}{dz} = \frac{1}{s\beta} (y^*)^{s+1} \left(1 - \frac{\beta}{(y^*)^s}\right)^{1-s} \simeq \frac{(y^*)^{s+1}}{s\beta}. \tag{23}$$

Thus

$$\left(\frac{dF}{dz}\Big|_{z=z^*}\right)^{-1} \equiv \left(\frac{dy^*}{dz}\right)^{-1} \simeq \frac{s\beta}{(y^*)^{s+1}}. \tag{24}$$

Finally, using (15), (18) and (24), we conclude that in the asymptotic regime $y^* \rightarrow \infty$ the tail of the distribution of the fixed points behaves as

$$P(y^*) \simeq \frac{s\beta}{\tau(y^*)^{s+1}} P_\lambda \left(\frac{\beta}{\tau(y^*)^s}\right). \tag{25}$$

In other words, the behaviour of $P_\lambda(\lambda)$ at $\lambda \rightarrow 0$ determines the tail of the distribution of the fixed points: If $P_\lambda(\lambda)$ goes to a non-zero value or goes to zero sufficiently slow, or even if it mildly diverges, the fixed point distribution has a long tail.

Note that this approach is valid only if $s \geq 1$ and Φ assumes, at least asymptotically, the form (20). Should $\Phi(y)$ have this form for *all* values of y , some additional constraints for the polynomials $S(y)$, $Q(y)$, $R(y)$ must be specified in order for the map (11) to have a stable fixed point and to be always positive provided the sequence of $\{y_n\}$ starts from a nonnegative number. For instance, if $\Phi(y)$ takes the form

$$\Phi(y) = \frac{y}{1 + \alpha y^{m+\eta}} \tag{26}$$

with $m \geq 1$, $0 \leq \eta < 1$, and $\alpha > 0$, which belongs to the general class (20), the map (11) (a) assumes only positive values provided it starts from a positive value, (b) has a fixed point at $y^{(0)} = 0$, and (c) for ε larger than the threshold value

$$\varepsilon > \varepsilon_{\text{threshold}} = e^{\lambda\tau} - 1, \tag{27}$$

has a unique stable and positive fixed point. We are not saying, though, that (26) is the most general form of $\Phi(y)$ to guarantee this.

We now apply the above formalism to our two models A, B.

3.1. Model A

With $\Phi = 1$, (11) reads

$$y_{n+1} = e^{-\lambda\tau} y_n + \varepsilon. \tag{28}$$

This map has a fixed point

$$y^* = \frac{\varepsilon}{1 - e^{-\lambda\tau}}, \tag{29}$$

which is always stable and attracting. For the distribution of the fixed points we obtain

$$P(y^*) = \frac{\varepsilon y^*}{\tau(y^* - \varepsilon)(y^*)^2} P_\lambda \left(-\frac{1}{\tau} \ln \left(1 - \frac{\varepsilon}{y^*} \right) \right), \tag{30}$$

and in the limit $y^* \rightarrow \infty$ (30) becomes

$$P(y^*) \simeq \frac{\varepsilon}{\tau(y^*)^2} P_\lambda \left(\frac{\varepsilon}{\tau y^*} \right). \tag{31}$$

As we can see, the asymptotic behaviour of $P(y^*)$ with $y^* \rightarrow 0$ is determined by the behaviour of $P_\lambda(\lambda)$ at $\lambda \rightarrow 0^+$. If $P_\lambda(\lambda) \sim \lambda^\nu$ for $\lambda \rightarrow 0^+$ with $\nu > -1$ (otherwise $P_\lambda(\lambda)$ would not be normalizable),

$$P(y^*) \sim \frac{\text{const}}{(y^*)^{2+\nu}}, \quad y^* \rightarrow \infty. \tag{32}$$

Thus, any distribution of $P_\lambda(\lambda)$ that is singular for $\lambda \rightarrow 0$ ($-1 < \nu < 0$) or has a finite value at $\lambda = 0$ (like a uniform or an exponential distribution) will induce a long-tail distribution $P(y^*)$ such that all moments of $P(y^*)$ diverge.

3.2. Model B

With Φ given by (8), (11) becomes

$$y_{n+1} = e^{-\lambda\tau} \left(y_n + \frac{\varepsilon y_n}{1 + \alpha e^{-\lambda\tau} y_n} \right). \tag{33}$$

Unlike the map (28), the map (33) has two fixed points:

$$y^{(0)} = 0 \quad \text{and} \quad y^* = \frac{(1 + \varepsilon)e^{-\lambda\tau} - 1}{\alpha e^{-\lambda\tau}(1 - e^{-\lambda\tau})}. \tag{34}$$

$y^{(0)}$ is stable only for ε below the threshold value

$$\varepsilon_{\text{threshold}} = e^{\lambda\tau} - 1. \tag{35}$$

Conversely, y^* is stable for all ε above the threshold value (35) and unstable below. In other words, for given values of λ and τ , ε must be large enough for y^* to be stable. The same statement can also be formulated as follows: $y^{(0)}$ is stable (y^* is unstable) for

$$e^{-\lambda\tau} < \frac{1}{1 + \varepsilon}, \tag{36}$$

and $y^{(0)}$ is unstable (y^* is stable) for $\lambda, \tau, \varepsilon$ not satisfying the inequality (36).

It is easy to verify that a stable fixed point of the map (33) is also an attracting point: any sequence $\{y_n\}_{n=0}^\infty$ starting with a positive y_0 will in the limit $n \rightarrow \infty$ either go to $y^{(0)}$ if the inequality (36) holds or to y^* otherwise. The situation where y_n goes to $y^{(0)}$ is usually termed “oscillator death”. As we shall see, the principal difference between models A and B lies in the fact that in the latter case the oscillators may “die” while in the former they always go to a positive resting point.

The probability of the oscillator death is equal to the probability of $y^{(0)}$ being stable:

$$P_0 = \text{Prob}(y^{(0)} \text{ stable}) = \int_0^{1/(1+\varepsilon)} P_z(z) dz = \int_{\ln(1+\varepsilon)/\tau}^\infty P_\lambda(\lambda) d\lambda. \tag{37}$$

Similarly, the probability of y_n going to y^* , or the oscillator survival, is given by

$$P_* = \text{Prob}(y^* \text{ stable}) = 1 - P_0 = \int_0^{\ln(1+\varepsilon)/\tau} P_\lambda(\lambda) d\lambda. \tag{38}$$

For the distribution of the non-zero resting (fixed) points we get:

$$P(y^*) = \frac{1}{z^* \tau} \frac{\alpha(z^*)^2(1 - z^*)^2}{(1 + \varepsilon)(z^*)^2 - 2z^* + 1} P_\lambda\left(-\frac{\ln z^*}{\tau}\right), \tag{39}$$

where

$$z^* = \frac{\sqrt{(1 + \varepsilon - \alpha y^*)^2 + 4\alpha y^*} - (1 + \varepsilon - \alpha y^*)}{2\alpha y^*}. \tag{40}$$

Note, however, that unlike in the model A, with $P(y^*)$ given by (39), we have $\int_0^\infty P(y^*) dy^* = P_* < 1$: As there is a possibility of oscillator death, $P(y^*)$ is not normalized to unity.

In order to find the asymptotic behaviour of the distribution (39) let us first observe that for $y^* \rightarrow \infty$, $z^* \simeq 1 - \varepsilon/(\alpha y^*)$. Thus

$$P(y^*) \simeq \frac{\varepsilon}{\alpha\tau(y^*)^2} P_\lambda\left(\frac{\varepsilon}{\alpha\tau y^*}\right). \tag{41}$$

We can see that in the regime $y^* \rightarrow \infty$, the fixed points distribution (41) has exactly the form of (32), but with ε scaled by $1/\alpha$. The asymptotic expansion (32) is, consequently, valid for the model B as well. This results from the fact that in the limit $y \rightarrow \infty$ the model (8) reduces to the model (7) with ε scaled as above.

3.3. Both λ and τ random

If we consider a collection of non-interacting oscillators, we may admit that replicates differ not only in λ , but also in the times between external stimuli, τ (cf. Section 2 above). Because of the symmetry between λ and τ in (12), everything that has been said in the preceding subsection can be immediately translated to the case of λ fixed and τ random. Now assume that λ is drawn randomly from a distribution $P_\lambda(\lambda)$, and τ is drawn randomly from a distribution $P_\tau(\tau)$; we further assume that they are independent. Because both λ and τ are positive, their respective distributions must vanish for negative arguments. For the distribution of z (12) we now obtain

$$\begin{aligned}
 P_z(z) &= \int_0^\infty \int_0^\infty d\lambda d\tau \delta(e^{-\lambda\tau} - z) P_\lambda(\lambda) P_\tau(\tau) \\
 &= \int_0^\infty \frac{d\tau}{\tau z} P_\tau(\tau) P_\lambda\left(-\frac{\ln z}{\tau}\right). \tag{42}
 \end{aligned}$$

It may appear that the above formula is not symmetric in P_λ and P_τ . This lack of symmetry is, in fact, superficial: a simple change of variables in (42) interchanges the roles of P_λ and P_τ . Note that unlike in the case of only one of λ , τ being random, $P_z(z)$ given by (42) may be singular at $z \rightarrow 1$ even though both P_λ and P_τ are nonsingular.

In the model A, the distribution of the fixed points is given by

$$P(y^*) = \frac{\varepsilon}{(y^*)^2} P_z\left(1 - \frac{\varepsilon}{y^*}\right). \tag{43}$$

Its asymptotic behaviour is determined by the behaviour of $P_z(z)$ at $z \rightarrow 1$.

In the model B, for the probabilities of the oscillator death and survival we get, respectively,

$$P_0 = \int_0^{1/(1+\varepsilon)} dz P_z(z) = \int_0^\infty d\lambda P_\lambda(\lambda) \int_{\lambda^{-1} \ln(1+\varepsilon)}^\infty d\tau P_\tau(\tau), \tag{44}$$

$$P_* = \int_0^\infty d\lambda P_\lambda(\lambda) \int_0^{\lambda^{-1} \ln(1+\varepsilon)} d\tau P_\tau(\tau). \tag{45}$$

The last equality results from the normalization of P_λ and P_τ . For the distribution of non-zero fixed points we obtain

$$P(y^*) = \frac{\alpha(z^*)^2(1 - z^*)^2}{(1 + \varepsilon)(z^*)^2 - 2z^* + 1} P_z(z^*) \tag{46}$$

with z^* defined by (40). Once again $\int_0^\infty P(y^*) dy^* = P_* < 1$. The asymptotic behaviour of $P(y^*)$ is given by

$$P(y^*) \sim \frac{\varepsilon}{\alpha(y^*)^2} P_z \left(1 - \frac{\varepsilon}{\alpha y^*} \right), \quad y^* \rightarrow \infty, \tag{47}$$

which is again of the form (43) with ε scaled by $1/\alpha$.

As we have seen, the maps A and B differ mainly in that the map A has only one fixed point, and the map B has two fixed points, one of which corresponds to the oscillator death. The asymptotic ($y^* \rightarrow \infty$) properties of both maps are identical. We stress the fact that the long tails in the distribution of non-zero fixed points result from the behaviour of $P_z(z)$ at $z \rightarrow 1$, which in turn corresponds in either λ , or τ , or both going to zero. It is, therefore, *not* the long tails in P_λ or P_τ that lead to the long tails in $P(y^*)$; rather than that, very regular and seen in many real-life applications behaviour of P_λ, P_τ at *zero* leads to long tails in $P(y^*)$. Examples presented in Table 1 show that distributions of parameters expected in many natural systems lead to distributions with divergent moments; note that in most cases the variance and even the mean of the resulting distribution are not properly defined. The second and third columns of this Table show what types of distributions of λ and τ lead to a particular tail in the distribution of the resting points shown in the first column.

3.4. Variation in other parameters

Variation in ε does not induce any “long-tail” distribution of $P(y^*)$, providing $P_\varepsilon(\varepsilon)$ does not exhibit such a behaviour. The arguments of the preceding subsections can be repeated to obtain

$$P(y^*) = \left(\frac{dF}{d\varepsilon} \right)^{-1} P(\varepsilon^*), \tag{48}$$

where $y^* = F(\varepsilon^*)$ (compare with (15)). Differentiating (14) with respect to ε we obtain

$$P(y^*) = \frac{(1 - z) - \varepsilon(d\Phi/dy)|_{y=zF(\varepsilon^*)}}{\Phi(zF)} P(\varepsilon^*). \tag{49}$$

In the large y^* limit $\Phi \rightarrow \text{const}$ for both models A and B, so that

$$P(y^*) \sim P(\varepsilon^*), \quad y^* \rightarrow \infty. \tag{50}$$

This shows that the tails of the distribution of y^* follow the asymptotic behaviour of ε .

As we have seen above, the main difference in the asymptotic behaviour between model A and model B is the scaling of ε by a factor α^{-1} . We can use this observation to extend the result (50) to the case of a quenched disorder in α . Thus, for any distribution $P_\alpha(\alpha)$ which is finite or mildly diverging, there will be a “long-tail” distribution of the resting points y^* , namely $P(y^*) \sim (y^*)^{-2}$, due to a change in variables in (50). However, in many practical applications α^{-1} (or ε/α) rather than α is likely to have a

Table 1

Tails of the distribution of fixed points $P(y^*)$ resulting from various distributions of λ and τ . Due to symmetry, entries can be interchanged between the second and third columns without affecting the first one. “Fixed” means that the corresponding parameter has a constant value across the population

Tail of $P(y^*)$	λ distribution	τ distribution
$\frac{\ln y^*}{(y^*)^{1+\eta}}$	$\frac{b^\eta}{\Gamma(\eta)} x^{-1+\eta} e^{-bx}$ $0 < \eta < 1$	$\frac{c^\eta}{\Gamma(\eta)} y^{-1+\eta} e^{-cy}$
$\frac{1}{(y^*)^{1+\eta}}$	$\frac{b^\eta}{\Gamma(\eta)} x^{-1+\eta} e^{-bx}$ $0 < \eta < 1$	Fixed
	$\frac{b^\eta}{\Gamma(\eta)} x^{-1+\eta} e^{-bx}$ $0 < \eta < 1$	Uniform
	$\frac{b^{m+1}}{\Gamma(m+1)} x^m e^{-bx}$ $0 < \eta = \min(m, n) + 1 < 1, m \neq n$	$\frac{c^{n+1}}{\Gamma(n+1)} y^n e^{-cy}$
$\frac{\ln y^*}{(y^*)^2}$	Uniform	Uniform
	Exponential	Uniform
	Exponential	Exponential
$\frac{1}{(y^*)^2}$	Uniform	Fixed
	Exponential	Fixed
	$\frac{b^{m+1}}{\Gamma(m+1)} x^m e^{-bx}$ $m > 0$	Uniform
$\frac{\ln y^*}{(y^*)^{2+m}}$	$\frac{b^{m+1}}{\Gamma(m+1)} x^m e^{-bx}$ $m > 0$	$\frac{c^{m+1}}{\Gamma(m+1)} y^m e^{-cy}$
		$m > 0$
$\frac{1}{(y^*)^{2+m}}$	$\frac{b^{m+1}}{\Gamma(m+1)} x^m e^{-bx}$ $m > 0$	Fixed
	$\frac{b^{p+1}}{\Gamma(p+1)} x^p e^{-bx}$ $m = \min(p, q) > 0$	$\frac{c^{q+1}}{\Gamma(q+1)} y^q e^{-cy}$

physical interpretation, and any regular distribution of α^{-1} yields a regular distribution of the resting points. In the rest of the paper we concentrate on the quenched disorder in λ .

4. Numerical results for the coupled case

In this Section we consider the effects of interactions between individual oscillators on the distribution of the resting points. As we have mentioned, we assume that interactions occur during or immediately after the pulses, and we start with the nearest neighbour coupling. In this case Eqns. (10) take the form

$$y_n(i) = z(i)y_{n-1}(i) + \varepsilon(i)\Phi(z(i)y_{n-1}(i)) - \frac{k}{2}(2z(i)y_{n-1}(i) - z(i-1)y_{n-1}(i-1) - z(i+1)y_{n-1}(i+1)). \quad (51)$$

Here the index i numbers the oscillators and k is the coupling constant. In model A the above equation can be written as

$$\vec{Y}_n = \mathbf{A}\vec{Y}_{n-1} + \vec{\varepsilon}, \quad (52)$$

where \mathbf{A} is the matrix resulting from (51), $\vec{Y}_n = [y_n(1), y_n(2), \dots, y_n(N)]^T$ and $\vec{\varepsilon} = \varepsilon[1, 1, \dots, 1]^T$. The fixed point can be found by solving

$$(\mathbf{1} - \mathbf{A})\vec{Y}^* = \vec{\varepsilon}. \quad (53)$$

The matrix $\mathbf{1} - \mathbf{A}$ is a tridiagonal matrix with elements

$$(\mathbf{1} - \mathbf{A})_{i,i} = 1 - (1 - k)z(i), \quad (54a)$$

$$(\mathbf{1} - \mathbf{A})_{i,i-1} = -\frac{k}{2}z(i-1), \quad (54b)$$

$$(\mathbf{1} - \mathbf{A})_{i,i+1} = -\frac{k}{2}z(i+1). \quad (54c)$$

Eq. (53) has a unique solution if the matrix $\mathbf{1} - \mathbf{A}$ is invertible. However, only solutions with all $y^*(i) > 0$ are physically meaningful, and this can be satisfied if the spectrum of $\mathbf{1} - \mathbf{A}$ lies in the right half-plane. $\mathbf{1} - \mathbf{A}$ is a random matrix, possibly very large, and the task of finding its spectrum is very demanding despite a simple algebraic structure of this matrix. Nevertheless, it is easy to find a simple condition which if fulfilled, guarantees that the spectrum lies in the right half-plane. Specifically, by the Gershgorin theorem [11] the real part of the spectrum of this matrix is bounded from below by $\min_i \{u_i\}$, where

$$u_i = 1 - (1 - 2k)z(i) - k(z(i-1) + z(i+1)). \quad (55)$$

If $\forall i: u_i > 0$, also $\min_i u_i > 0$, and it is straightforward to verify that $0 \leq k < 1$ is a necessary and sufficient condition for $u_i > 0$ to hold for all possible values of z —this is thus the range of the coupling constant in which physically meaningful solutions exist.

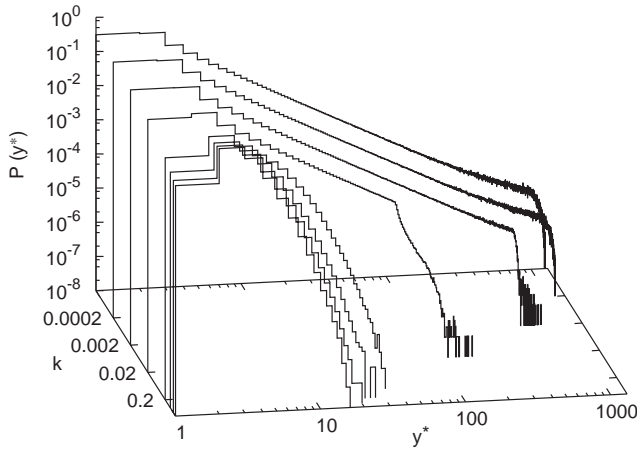


Fig. 1. Distribution of fixed points of the map (52). Parameter λ is drawn uniformly from the interval $[0, 1]$. Lines plotted correspond, back to front, to $k=0, 2 \times 10^{-4}, 2 \times 10^{-3}, 2 \times 10^{-2}, 0.2, 0.4, 0.6, 0.8$, respectively. Number of oscillators $N = 5 \times 10^5$, $\varepsilon = 1$.

Note that if $z(i) = z(i - 1) = z(i + 1) = 1$, $u_i = 0$, but as $z(i) \rightarrow 1$ only asymptotically, $z(i)$ can actually equal unity with zero probability; on the other hand, for $k \geq 1$, u_i may equal zero even if none of $z(i) = 1$. There is still a possibility that for a particular realization of the system all fixed points are positive (physical) even for $k \geq 1$; we have just shown that for $0 < k < 1$ the fixed points *must* be positive in all realizations.

Further analysis has been performed numerically. Instead of solving (53), we have directly run the map (52). The number of oscillators was $N = 5 \times 10^5$ and periodic boundary conditions have been used (for a large system the result differs only slightly from that with free boundaries). To make sure that all oscillators settled on their resting points, 10^3 iterations have been performed, and the resulting distribution has been averaged over 50 realizations. Fig. 1 shows histograms of the resting points distributions resulting from λ 's uniformly distributed in $[0, \Delta]$ with $\Delta = 1$. If the coupling constant vanishes, a clear $1/y^2$ tail is seen (a sharp drop for very large y is an artefact resulting from the sample being finite, as with the distribution of λ including 0 the distribution of y should extend to ∞). If the coupling is switched on, regions with power-law scaling persist for very weak couplings, but for k as little as 0.2 they disappear and the resting points cluster in a narrow band. Similar results have been obtained for different values of Δ (not plotted) and for λ 's drawn from different distributions. Fig. 2 show results for $P_\lambda(\lambda) = \lambda e^{-\lambda}$ —the only important difference is that the scaling exponent is now -3 , as expected. In each case studied the system became numerically unstable as soon as k approached unity, which signals the onset of unphysical behaviour.

For the model B with coupling, or the map

$$y_n(i) = y_{n-1}(i) + \varepsilon \frac{z(i)y_{n-1}(i)}{1 + \alpha z(i)y_{n-1}(i)} - \frac{k}{2} (2z(i)y_{n-1}(i) - z(i - 1)y_{n-1}(i - 1) - z(i + 1)y_{n-1}(i + 1)). \tag{56}$$

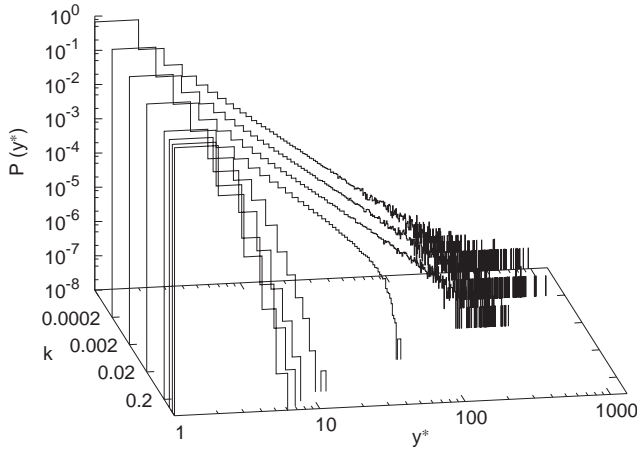


Fig. 2. Same as Fig. 1 but with λ drawn according to $P_\lambda(\lambda) = \lambda e^{-\lambda}$.

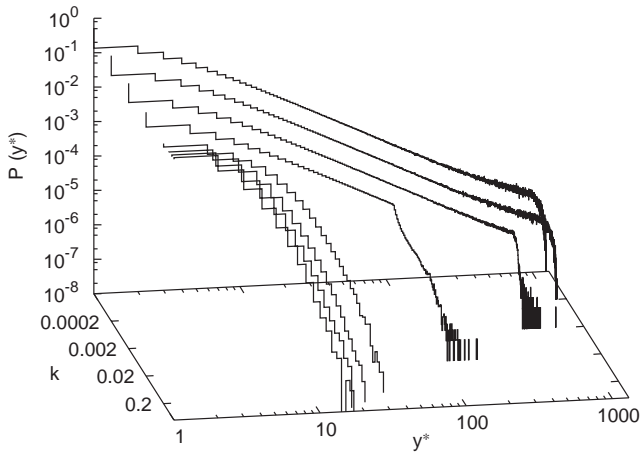


Fig. 3. Distribution of fixed points of the map (56). Parameter λ is drawn uniformly from the interval $[0, 1]$. Lines plotted correspond, back to front, to $k=0, 2 \times 10^{-4}, 2 \times 10^{-3}, 2 \times 10^{-2}, 0.2, 0.4, 0.6, 0.8$, respectively. Number of oscillators $N = 5 \times 10^5$, $\varepsilon = 1$, $\alpha = 1$.

no analytical results have been found. We have performed numerical simulations under the same conditions as for the model A, and the results are strikingly similar (cf. Fig. 3). The only difference is that while for the map (51) with λ 's uniformly distributed a clear maximum in $P(y^*)$ develops for $y^* > 1$, there is no such phenomenon in the map (56), which signals that a significant portion of the oscillators “die” or go to $y^{(0)} = 0$. Again, the system became numerically unstable for $k \simeq 1$. These results show that there is not much difference between the models A and B even with the coupling switched on. In both models the coupling of diffusive type tries to smooth

out differences between the replicates and if the coupling is large enough, it brings all the oscillators to a narrow band in the y space.

We now turn to the mean-field coupling. The coupled maps now become

$$y_n(i) = z(i)y_{n-1}(i) + \varepsilon - \frac{k}{N-1} \sum_{j=1}^N [z(i)y_{n-1}(i) - z(j)y_{n-1}(j)], \quad (57)$$

for the model A, and

$$y_n(i) = z(i)y_{n-1}(i) + \varepsilon \frac{z(i)y_{n-1}(i)}{1 + \alpha z(i)y_{n-1}(i)} - \frac{k}{N-1} \sum_{j=1}^N [z(i)y_{n-1}(i) - z(j)y_{n-1}(j)], \quad (58)$$

for the model B, respectively. The equation satisfied by the fixed points of (57) has the form (53) with

$$(\mathbf{1} - \mathbf{A})_{i,i} = 1 - (1 - k)z(i), \quad (59a)$$

$$(\mathbf{1} - \mathbf{A})_{i,j} = -\frac{k}{N-1} z(j), \quad j \neq i. \quad (59b)$$

Note that \mathbf{A} no longer is tridiagonal. By an argument similar as above, we can show that for $N \gg 1$ the spectrum of $\mathbf{1} - \mathbf{A}$ lies in the right half-plane, or that physically meaningful solutions exist, for $0 \leq k < 1$, exactly like in the previously discussed case. By numerically simulating the map (57) under conditions identical to those used above, we get results analogous to those of the map with the nearest neighbours coupling: For small couplings there are regions in which the power scaling persists. These regions disappear as the coupling increases and fixed points of the map (57) become confined to a narrow band, Fig. 4. However, while distributions obtained with the map (52) approached zero gradually, with quite pronounced fluctuations for large values of y^* , distributions obtained with the map (57) have sharp edges and are much narrower than in the previous case. Also the general shapes of the distributions differ (c.f. Fig. 5). This is a consequence of the fact that nearest neighbours coupling tries to smooth the system locally, and therefore affects mostly the points that deviate from their neighbours. In contrast, the mean field coupling has a global character and therefore will affect all points to the same extent.

Results with different values of Δ or with different $P_\lambda(\lambda)$ are also analogous to those discussed previously.

4.1. Cluster distribution and domain forming

When the coupling is switched on, the oscillators in a similar resting state can be localised in clusters in space (with a one-dimensional space represented here by the index i). In order to quantify the clustering, we define a domain as a compact set of oscillators for which the value of $y(i)$ exceeds an arbitrary threshold, y_c . Thus, inside

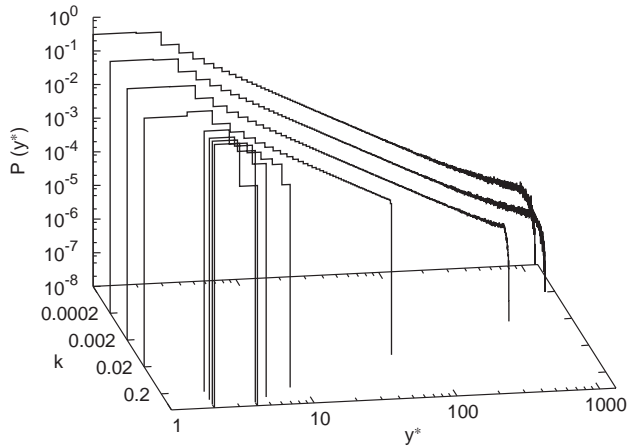


Fig. 4. Distribution of fixed points of the map (57). Parameter λ is drawn uniformly from the interval $[0, 1]$. Lines plotted correspond, back to front, to $k=0, 2 \times 10^{-4}, 2 \times 10^{-3}, 2 \times 10^{-2}, 0.2, 0.4, 0.6, 0.8$, respectively. Number of oscillators $N = 5 \times 10^5$, $\varepsilon = 1$.

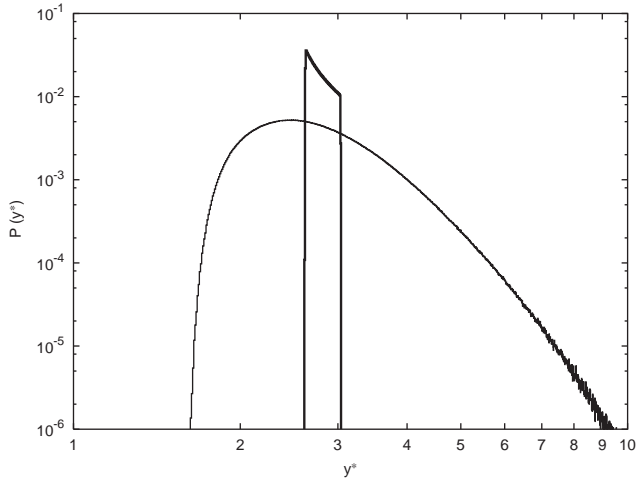


Fig. 5. Comparison of fixed point distributions in model A with mean field (heavy line) and nearest neighbours (thin line) coupling. Parameter λ is drawn uniformly from the interval $[0, 1]$. In each case number of oscillators $N = 5 \times 10^5$, $\varepsilon = 1$, the coupling constant $k = 0.8$.

a cluster at least one of the neighbours of an oscillator in a “high” state ($y(i) > y_c$) is also in the same state.

The pattern of alternating “high” and “low” domains is generated by two basic mechanisms. Simply thresholding a completely random distribution of resting states generates apparent clustering that should be, however, distinguished from an additional

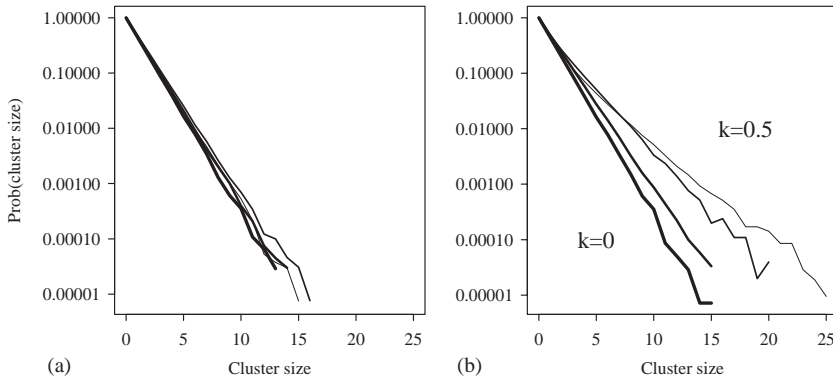


Fig. 6. Normalised distributions of cluster sizes in a one-dimensional realisation of the model with a global (a) and local (b) coupling. Note the logarithmic scale for $P(s)$. The width of the lines denotes varying levels of coupling from $k = 0$ (thick line) through $k = 0.025, 0.2$ to 0.5 (thin line). 10^6 oscillators, $y_c = 8$, $\varepsilon = 5$, $\alpha = 1$.

order introduced by coupling between neighbouring oscillators. In order to study the dependence of domain formation on coupling, these two factors must be separated.

We characterise the distribution of “high” and “low” oscillators by calculating the resting state of the array of oscillators for a given distribution of λ s and subsequently identifying oscillators belonging to “high” (“low”) clusters. Fig. 6 shows selected examples of cluster size distributions for different values of coupling. The distributions are approximately exponential for the whole range of a coupling constant. The probability of observing a cluster with a size s is thus given by $P(s) \sim \exp(-s/\sigma)$. A characteristic size of a cluster, σ , can then be estimated from the simulated data as a slope of the straight-line relationship between $\log(P(s))$ and s , as in Fig. 6. σ can also be interpreted as an average cluster size. Simulations presented here have been performed for the model B.

In the case when there is no coupling, cluster size distribution reflects directly the quenched disorder in the parameters. In this case, σ can be related to the average density of oscillators in the “high” state in the following way: Assuming no correlation between neighbouring oscillators, the probability of having a “high” oscillator next to a given oscillator equals the proportion of “high” oscillators to the total number, $p \equiv N_{\text{high}}/N_{\text{total}}$. If the “high”/“low” states are allocated randomly and independently, the probability of having s “high” oscillators in a cluster is p^s . Thus, the probability of creating a cluster of exactly size s is equal to $p^s(1-p)^2$ (the factor $(1-p)^2$ corresponding to having two “low” oscillators at two ends). Reparametrising this formula we obtain $\exp(-s/\sigma_0) = p^s(1-p)^2$, so that the characteristic length in the uncoupled case, σ_0 is given by $\sigma_0^{-1} = -\log(p)$.

By comparing the actual (fitted) values of σ to σ_0 we can quantify the effects of the coupling on the formation of the domains. In particular, large values of σ (or $\sigma/\sigma_0 \gg 1$) correspond to high levels of spatial correlation between the oscillators, significantly exceeding potential “random” correlations resulting purely from the underlying quenched disorder.

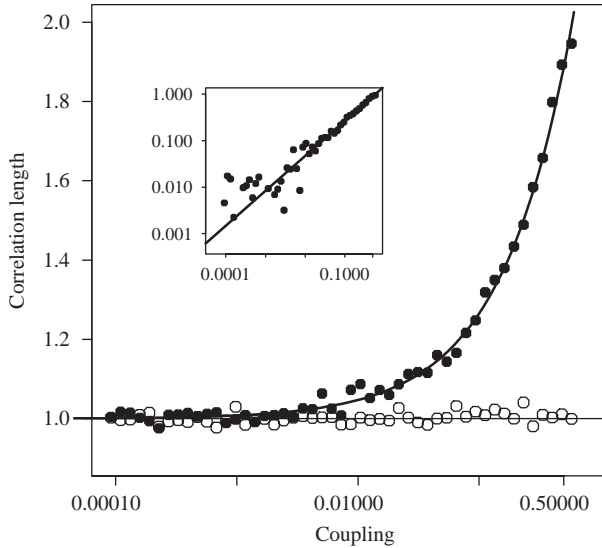


Fig. 7. A ratio between the characteristic correlation length of the cluster size distribution, σ , and the value corresponding to a completely random distribution, as a function of a coupling constant, k . Closed circles correspond to the local coupling, and open circles to the global coupling. The inset shows a plot of $(\sigma/\sigma_0) - 1$ versus k on a double-logarithmic scale, with a straight line corresponding to a power law, $\sigma/\sigma_0 = 1 + 1.492k^{0.75}$ —also shown as a curve on the main graph.

Fig. 7 shows the dependence of σ/σ_0 on the coupling constant k . The ratio is independent of the threshold in a wide range of y_c , providing y_c falls within a support of a distribution of the resting states (see e.g. Fig. 5). For any value of the global coupling and for low values of the local coupling, the distribution of the resting states is dominated by the differences between oscillators rather than non-local effects, and therefore is completely random, $\sigma/\sigma_0 \simeq 1$. Under this assumptions, the clustering is generated purely by the underlying quenched disorder.

For higher values of the local coupling, domains of highly correlated oscillators are formed by the interactions and therefore $\sigma/\sigma_0 \gg 1$, see Fig. 7. Even then, however, the correlation length is relatively small (only twice as large as for a purely random pattern), and so the clustering pattern is still dominated by the quenched disorder rather than by the coupling. The characteristic correlation length for the local coupling appears to follow a power law (see also an inset in the figure).

5. Possible applications

Although the primary purpose of the present paper is to discuss the mathematical formalism involved, in this section we briefly mention some of its possible applications.

Systems discussed in this paper come out as natural models for many biological and ecological processes. Suppose for example that $y(t)$ gives the density (numbers) of parasites within an individual. New parasites are introduced at (almost) regular intervals through eating or drinking contaminated water—these correspond to the external stimuli in our model. Between the intakes, parasites are removed from the organism and so their number decays. The resting point distributions from Sections 3 and 4 now describe the distribution of the parasites within individuals drawn from a population. Results presented here might be thus helpful in understanding overdispersion noted in parasite burden in some human or animal diseases [12]. The same model may also describe dynamics of a seed-bank for an annual plant population in the presence of environmental variability and dispersal. A slight modification of the model leads to a proper description of a competition between two or more species. These issues will be discussed in detail elsewhere [13].

Our model has also a very simple yet interesting interpretation in terms of econophysics [14]. Consider a group of people in receipt of regular payments ε (salary or benefits) which are uniform across the population and arriving at time $t = n\tau$ (say, monthly). The funds are then spent throughout the month, at a rate proportional to the current account balance. The latter assumption can be relaxed as long there is a monotonic relationship of the balance before the payment at the end of the month to the balance at the beginning of the same month (after the payment). The rate λ varies between people according to some simple and bounded probability distribution. The resulting distribution of wealth (characterised by a balance y_n after the payment each month) is highly skewed with the tail described by a power law y^{-2} . High levels of dispersion are easy to understand as individuals who spent particularly slowly are able to accumulate funds relatively quickly. We also note that in order to increase an overall wealth of a society, people should be encouraged to spend less (decrease in λ) rather than be offered a larger income (increase in ε). The coupling (wealth transfer), proportional to the difference in savings limits the excesses of the wealth accumulation, but initially affects only the tails of the distribution. In real applications there are more nonlinearities as agents with more funds can invest proportionally more and therefore obtain a higher return.

It is also perhaps interesting to note that maps similar to ours have been studied in the context of the Frenkel–Kontorova model [15], to which our model bears some formal similarity.

6. Discussion

We have shown that for a wide class of maps the disorder in some parameters may lead to long-tail distributions of the fixed points. Such behaviour can be expected for many distributions of parameters believed to occur in many natural systems: uniform, Poisson, exponential, χ^2 and many others that do not vanish fast enough for *small* arguments. It is not tails of the underlying distributions of parameters that lead to the long tails in the distributions of the fixed points; rather than that, distributions that may differ wildly in their tails but behave similarly for small

arguments, lead to identical tails in the distribution of the fixed points. A universality of a power law that is not a part of the model construction is an interesting feature. On the level of mathematical formalism used, this universality is a consequence of a nonlinear change of variables needed to transform our problem from one stochastic variable, λ , to another variable, $z = e^{-\lambda\tau}$. It is interesting to note that a similar approach has been recently used in Ref. [16], where long tails in temporal correlations also resulted from a nonlinear transformation between various stochastic variables.

We have also shown that two models discussed here in detail, (7) and (8), which differ for small arguments but share a similar behaviour in the asymptotic regime, lead to similar distributions of the fixed point. The principal difference between these models is that the latter has two fixed points and there is a probability that some oscillators will “die”, or go to the trivial fixed point $y^{(0)} = 0$. All qualitative results valid for (8) are also valid for (26).

In the coupled case, for model A we have analytically established a range of admissible couplings, that is to say, the couplings that lead to physically meaningful solutions. In model B our numerical results strongly suggest that admissible coupling are the same as in model A. This once more confirms that there is little difference between models A and B. The interactions destroy the power law scaling seen in the uncoupled case. These results are in contrast with those of Ref. [7], where interactions facilitated the emergence of long-tail distributions, but this difference can be explained by two factors: First, there was no external stimulation in Ref. [7], and the external stimulation plays a crucial role in the dynamics of the present system. Second, Biham et al. have used multiplicative coupling of individual agents with the mean, while in our case the coupling is of diffusive type and tends to smooth out any differences between the individual oscillators.

We also looked at formation of domains of oscillators by introducing a threshold into a distribution of the fixed points of the oscillators. We introduced a method of spatial pattern analysis that can distinguish between an apparent clustering reflecting the randomness of the quenched disorder and the effects of interactions between the oscillators. Small levels of coupling (either global or local) affect the peaks of the resting states within the clusters, but the distribution of cluster sizes is largely unaffected by the coupling and follows an exponential (Poisson) distribution. For the global coupling, this holds for all levels of coupling. With the strength of the local coupling increasing, the power-law distribution of resting states within “high” clusters is first distorted and then disappears, although the cluster sizes are still largely random. For still higher values of local coupling, large domains start to appear, but at this point the power-law distribution of the peaks is already destroyed (compare the values of coupling in Fig. 1 and Fig. 7). The distribution and dynamics of clusters deserve a separate study, and we will address it in future papers.

Finally, we note that the nearest neighbours coupling admits a greater degree of disorder than coupling of the mean field type. It will be interesting to see how additional interactions, between second, third etc. neighbours, or between oscillators coupled randomly, change the domains by introducing additional smoothing.

Acknowledgements

The work was funded in part by a King's College Senior Research Fellowship and by the BBSRC (AK) and by the Polish-British Joint Research Collaboration Programme (AK and PFG), which we gratefully acknowledge.

References

- [1] Per Bak, Kim Christensen, Leon Danon, Tim Scanlon, *Phys. Rev. Lett.* 88 (2002) 178 501.
- [2] A.L. Barabási, R. Albert, *Science* 286 (1999) 509;
S.N. Dorogovtsev, J.F.F. Mendes, A.N. Samukhin, *Phys. Rev. Lett.* 85 (2000) 4633;
F. Slanina, M. Kortla, *Phys. Rev. E* 62 (2000) 6170.
- [3] P.M. Gade, C.-K. Hu, *Phys. Rev. E* 60 (1999) 4966;
S. Jespersen, A. Blumen, *Phys. Rev. E* 62 (2000) 6270.
- [4] C. Moore, M.E.J. Newman, *Phys. Rev. E* 62 (2000) 7059.
- [5] N. Vandewalle, J.F. Lentz, S. Dorbolo, F. Brisbois, *Phys. Rev. Lett.* 86 (2001) 179.
- [6] K. Okuyama, M. Takayasu, H. Takayasu, *Physica A* 269 (1999) 125;
J.J. Ramsen, *Physica A* 277 (2000) 200.
- [7] O. Biham, O. Malcai, M. Levy, S. Solomon, *Phys. Rev. E* 58 (1998) 1352.
- [8] I.R. Epstein, *Nature (London)* 374 (1995) 321;
A. Kleczkowski, D.J. Bailey, C.A. Gilligan, *Proc. R. Soc. Lond. B* 263 (1996) 777.
- [9] A. Kleczkowski, *Acta Phys. Polon. B* 24 (1993) 1061;
A. Kleczkowski, *Acta Phys. Polon. B* 24 (1993) 1445.
- [10] P. Reimann, P. Talkner, in: P. Talkner, P. Hänggi (Eds.), *New Trends in Kramers' Reaction Rate Theory*, Kluwer, Amsterdam, New York, 1995.
- [11] G.H. Golub, C.F. Van Loan, *Matrix Computations*, The John Hopkins University Press, Baltimore, 1983.
- [12] M.E.J. Woolhouse, in: V. Isham, G. Medley (Eds.), *Models for Infectious Human Diseases: Their Structure and Relation to Data*, Cambridge University Press, Cambridge, 1995;
D. Shaw, A. Dobson, *Parasitology* 111 (1995) S111;
J. Herbert, V. Isham, *J. Math. Biol.* 40 (2000) 343.
- [13] A. Kleczkowski, P.F. Góra, unpublished.
- [14] R.N. Mantegna, H.E. Stanley, *An Introduction to Econophysics*, Cambridge University Press, Cambridge, 1999.
- [15] S.N. Coppersmith, *Phys. Rev. A* 36 (1987) 3375;
S.N. Coppersmith, *Phys. Rev. A* 38 (1988) 375.
- [16] M.O. Vlad, F.W. Schneider, J. Ross, *Physica A* 294 (2001) 1.